Circuit Models of the Passive Electrical Properties of Frog Skeletal Muscle Fibers

R. VALDIOSERA, C. CLAUSEN, and R. S. EISENBERG

From the Department of Physiology, University of California at Los Angeles, Los Angeles, California 90024

ABSTRACT The relation between the fine structure, electric field equations, and electric circuit models of skeletal muscle fibers is discussed. Experimental evidence illustrates the profound variation of potential with circumferential position, even at low frequencies (100 Hz). Since one-dimensional cable theory cannot account for such variation, three-dimensional cable theory must be used. Several circuit models of a sarcomere are presented and plots are made of the predicted phase angle between sinusoidal applied current and potential. The circuit models are described by equations involving normalized variables, since they affect the phase plot in a relatively simple way. A method is presented for estimating the values of the circuit elements and the standard deviation of the estimates. The reliability of the estimates is discussed. An objective measure of fit, Hamilton's R test, is used to test the significance of different fits to data. Finally, it is concluded that none of the proposed circuit models provides an adequate description of the observed variation of phase angle with circumferential location. It is not clear whether the source of disagreement is inadequate measurements or inadequate theory.

The flow of current in a cylindrical cell like a muscle fiber has often been analyzed by representing the cell as an equivalent circuit of resistors, capacitors, and wires (Bozler and Cole, 1935; Falk and Fatt, 1964; Eisenberg, 1967; Freygang et al., 1967; Schneider, 1970; see reviews by Jack et al., 1973; Peachey and Adrian, 1973). The adequacy of the circuit model can be tested by comparing, over a wide range of frequencies, the impedance predicted by the model with the impedance actually observed. The values of the circuit elements which give the best fit between the predicted impedance and that actually measured are interpreted as the intrinsic electrical properties of the corresponding structural elements of the muscle fiber.

There are several ambiguities in this kind of circuit analysis besides the obvious ones produced by the limited range and accuracy of experimental

data. There are a finite number of circuits with the same number of elements which have precisely the same impedance at all frequencies and an infinite number of such circuits with additional elements.[1] Most such circuits are incompatible with the fine structure of a muscle fiber and so can be rejected. It is much more difficult to distinguish between circuits with approximately the same impedance, but the different values of corresponding circuit elements in such circuits can be exploited (see Valdiosera et al., 1974 *b*).

The relation between these circuit models and the structure of the muscle fiber is less direct than it seems. In order to make precise predictions concerning the expected electrical properties of a complicated structure it is necessary to solve the partial differential equations which specify the electric field in that structure. It seems unlikely that the full set of equations for a muscle fiber will be solved in the immediate future. Indeed it is only recently that the problem of a microelectrode source in a spherical cell has been solved completely (Peskoff et al., 1972) and the cylindrical cell still has only been solved in a restricted case (Peskoff et al., 1973). In order to make predictions one must then resort to circuit models consisting of resistors, capacitors, and wires and other heuristic and "irrational" approximations (irrational in the sense that the approximations do not permit the calculation of a bound on their own error: see van Dyke, 1964, Chap. 1). These approximations cannot in general account for all the properties of the original set of partial differential equations or of the muscle fiber, and one must expect difficulties and anomalies from circuit models, especially in regions where the potential may vary steeply, at source points or near boundaries. The approach that has been taken is to make a series of circuit approximations to a muscle fiber, each incorporating features to account for difficulties and anomalies, with the hope that enough intuition and physical insight can substitute for a complete solution of the partial differential equations.

We will consider in this paper a series of electrical models of a muscle fiber, each one of which has a simple interpretation in terms of the structure of frog muscle fibers as described by Peachey (1965). The essential simplification which underlies our treatment was introduced by Falk and Fatt (1964) and elucidated and extended by Adrian, Chandler, and Hodgkin (1969) and Schneider (1970). These authors considered the muscle fiber to be composed of essentially three electrical components: a longitudinal resistance, r_i, residing presumably in the sarcoplasm, a shunt admittance $\mathbf{y}_T$,[2] representing the passive electrical pathways by which current can flow

[1] It is not always realized that while the input-output relations of different equivalent circuits are identical, the values of the circuit parameters are not identical. For example, the total capacitance (the sum of the value of all the capacitors in the circuit) is *not* the same in different equivalent circuits.

[2] We use the standard convention of electric circuit theory and represent currents voltages, admittance, and impedances by complex variables printed in bold-face type (Desoer and Kuh, 1969, Chap. 7).

into the tubular system and out of the fiber, and the shunt admittance of the surface membrane itself. The arrangement of these electrical components and their relation to the structure of the muscle fiber are shown in Fig. 1.

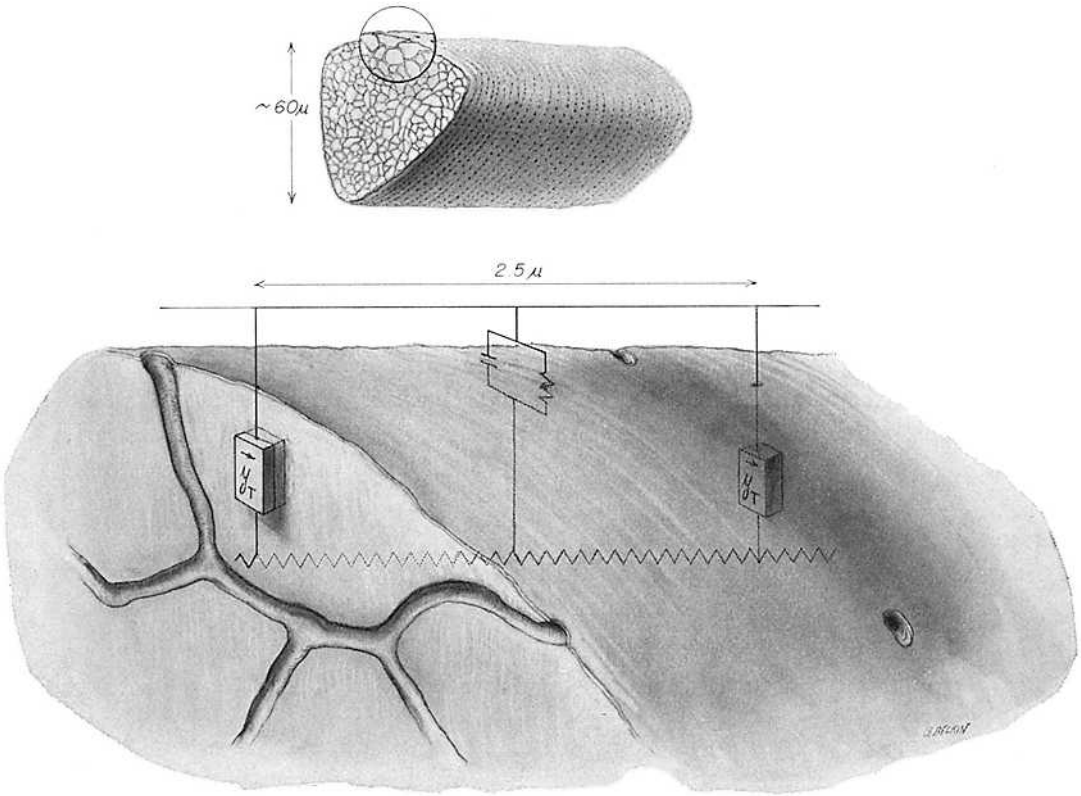

FIGURE 1. The relation between the circuit model and the structure of a muscle fiber. The electrical properties of the muscle fiber are presumed to arise in three structures: the surface membrane, the sarcoplasm, and the tubular system. The surface membrane is represented as a parallel combination of the resistance r_m and the capacitance c_m. The sarcoplasm is represented here as a resistance r_i, although consideration of the circumferential and radial variation of potential near the current microelectrode requires a more complex representation (see text and Figs. 2 and 7). The tubular system is represented by an admittance $\mathbf{y}_T$, various models for which are described in the text. The sarcoplasmic reticulum is not included in the figure or circuit since there is little evidence that it has a significant effect on passive electrical properties. (In figure μ = μm.)

The density of the components is quite high, at least in the longitudinal direction, and so the repeating structure has been approximated by a continuous distributed transmission line, a one-dimensional electrical cable. The separation of the electrical properties of a muscle fiber into these components considerably simplifies the theory since it circumvents the problem of solving the complete set of partial differential equations.

In all these circuit models the entire variation of potential is ascribed to the unidirectional longitudinal flow of current down the resistance of the sarcoplasm; there is assumed to be no radial or circumferential flow of current in the sarcoplasm itself. In several of the circuit models of the tubular system (Falk and Fatt, 1964, Appendix D; Adrian, Chandler, and Hodgkin, 1969, Schneider, 1970; Peachey and Adrian, 1973) radial, but *not* circumferential, potential gradients are allowed in the lumen of the tubules, but are not allowed in the sarcoplasm. Thus, one solves the equations for current flow in the longitudinal direction by one-dimensional cable theory and then one separately solves the equations which are supposed to describe the radial flow of current in the lumen of the tubular system. The two solutions can be obtained essentially independently since they are not intimately coupled, the only relation being conservation of current; that is to say, the current leaving the sarcoplasm in the longitudinal equations must equal the sum of the current flowing across the surface membrane and the current flowing radially in the tubular system.

In this paper we will first describe experimental results which indicate the importance of the circumferential and radial potential gradients in the sarcoplasm and will show how to include the effects of such gradients, at least to a first approximation, in circuit models. We then will introduce a variety of circuit models and illustrate their passive electrical properties; in order to do this we introduce a new set of normalized variables. A method is presented for determining the values of the parameters of a circuit model which produces the "best" fit between the theoretically predicted and experimentally determined impedance; statistical estimates of the accuracy of the fit and of the precision of the parameter values are also given. Finally, we discuss likely errors in the electric circuit models themselves.

RESULTS

Circumferential Variation of Potential: Experimental Evidence

The electrical models of muscle fibers considered to date have used one-dimensional cable theory to describe the spread of potential in muscle fibers. There are a number of theoretical papers which claim, however, that circumferential and radial potential gradients should exist and be significant in cylindrical muscle fibers (Eisenberg and Johnson, 1970; Barcilon et al., 1971; Peskoff et al., 1972, 1973; a review of the literature can be found in Peskoff and Eisenberg, 1973). There are some indirect indications of circumferential and radial potential gradients in the experiments of Adrian, Costantin, and Peachey (1969) and Costantin (1970) but there has been no direct experimental evidence concerning the existence of these effects, let alone their quantitative significance, and so we thought it worthwhile to seek such evidence.

Impedance measurements were made by the techniques described by Valdiosera et al., 1974 *a*. Measurements were made at two different circumferential positions of the voltage microelectrode, the longitudinal position being constant, and the radial position being unknown. The results shown in Fig. 2 are selected from many experiments which illustrate the existence

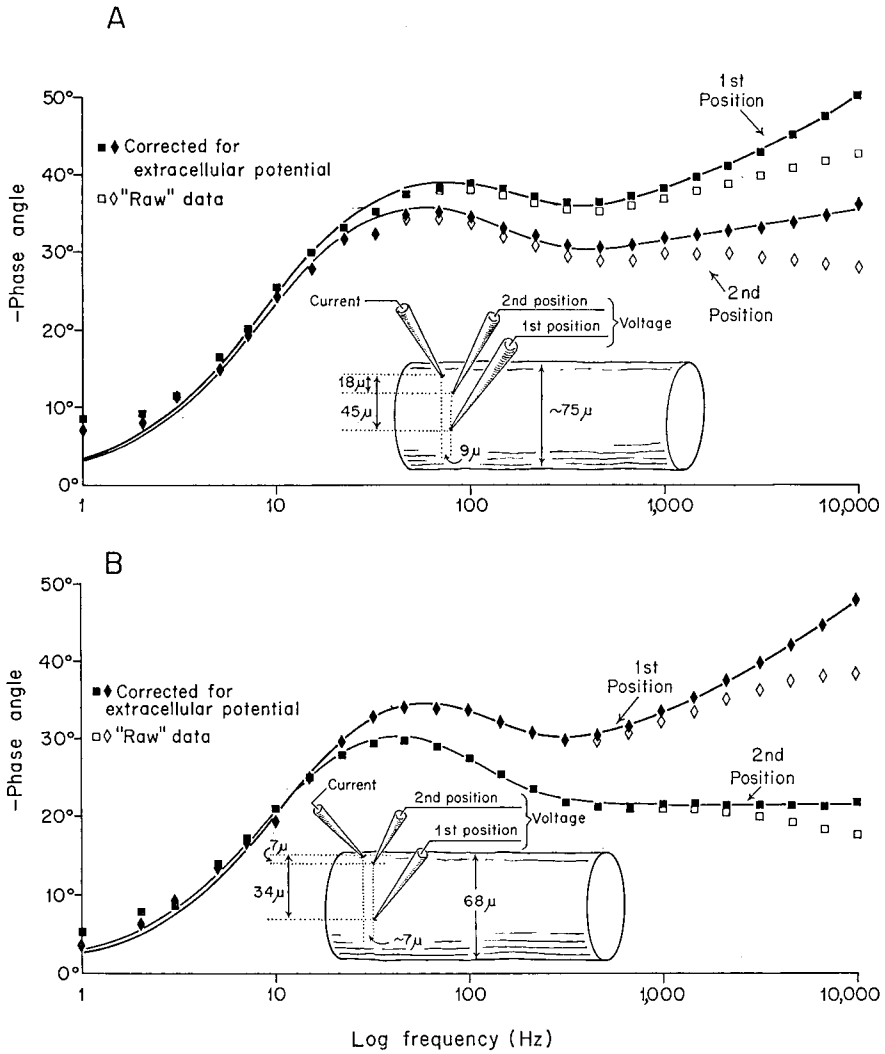

FIGURE 2. The circumferential variation of phase angle. The results of experiments on muscle fibers in which the voltage microelectrode was moved circumferentially around the fibers. The approximate positions of the electrodes and "diameter" of the fibers are shown, although the depth of the microelectrode and shape of the fibers are not known. Note that there is a profound radial variation of phase angle and thus potential even at low frequencies. Since one-dimensional cable theory cannot account for such effects, it is necessary to use three-dimensional cable theory even at quite low frequencies. (In figure μ = μm.)

of a circumferential variation of potential; the criterion for selection was stability of the resting potential and of the impedance observed at a frequency of 10 Hz. The approximate positions of the microelectrodes are shown as observed with a compound polarizing microscope at a magnification of some × 375. The open points are the raw experimental data, corrected only for phase errors in the recording apparatus. The filled points are data corrected for the measured extracellular potential. The solid lines are theoretical curves discussed below. Note that in each case there is a profound variation of phase angle with electrode location even at low frequencies. It is necessary then to include the possibility of circumferential variation of potential when the electrical properties of cells are measured by the application of current from a microelectrode.

Circumferential Variation of Potential: Theoretical Model

The question then is how can one include the effects of the circumferential potential gradient, which we will call a local potential for short, without destroying the simplicity of a circuit model of the fiber. The original analyses of the local potential (Weinberg, 1942; Falk and Fatt, 1964; Eisenberg, 1967; Adrian, Costantin, and Peachey, 1969) seem somewhat complex and not amenable to physical interpretation, but the approximate treatment of Eisenberg and Johnson, 1970, reduced the complexity of the problem. Recent results using singular perturbation theory (Peskoff et al., 1973) provide a simple physical interpretation of the local potential and its interaction with the potential given by the usual expressions of one-dimensional cable theory. The local potential adds to the potential in the far field, the region away from the point source, without interaction. The total observed potential can then be written as:

$$\frac{V(\mathbf{r}, \mathbf{R}; a, \mathbf{y}, r_i)}{i_o/2} = L(x; \underline{r}, r_i, \mathbf{y}) + r_i a S(\mathbf{r}, \mathbf{R}), \quad (1)$$

where

$$L(x; \underline{r}, r_i, \mathbf{y}) = (r_i/\mathbf{y})^{1/2} e^{-x(r_i \mathbf{y})^{1/2}}, \quad (2)$$

where V(**r**, **R**; a, **y**, r_i) is the potential observed at position **r** with a point source at **R**; i_o = the current applied (amperes); $\underline{r}$ = the shunt resistance in a unit length of fiber, including the resistance of surface and tubular membranes (ohm-centimeter); r_i = the resistance of a unit length of sarcoplasm (ohm/centimeter); **y** = the shunt admittance, which depends on frequency of a unit length of fiber (mho/centimeter); a = the fiber radius (centimeter); x = the longitudinal position of the voltage microelectrode (centimeter); S(**r**, **R**) is the variable defined by Eisenberg and Johnson (Eq. IV. 3-3, p. 24, 1970) to describe the local potential.

This equation can be derived from the analysis of Eisenberg and Johnson (loc. cit.) or from Eq. 5.3 of Peskoff et al. (1973) by the method described in Appendix 2 of Eisenberg and Engel (1970). The equation can be simplified in the case where the two microelectrodes are close together by expanding the exponential in a Taylor series (Eisenberg and Johnson, 1970, p. 58):

$$\frac{V(\mathbf{r}, \mathbf{R}; a, \mathbf{y}, r_i)}{i_o/2} = (r_i/\mathbf{y})^{1/2} + (\underline{r}r_i)^{1/2} P(\mathbf{r}, \mathbf{R}; a, \lambda), \tag{3}$$

where the proximity variable is defined for computational convenience as

$$P(\mathbf{r}, \mathbf{R}; a, \lambda) = \frac{a}{\lambda} S(\mathbf{r}, \mathbf{R}) - \frac{x}{\lambda} + \cdots, \tag{4}$$

where $\lambda = (r/r_i)^{1/2}$.

The terms shown in Eq. 4 are sufficient if $| x(r_i\mathbf{y})^{1/2} | \ll 1$. In a typical case, as illustrated in Fig. 7, $| x(r_i\mathbf{y})^{1/2} | \sim \omega^{1/2} x \cdot$ (0.31 s/cm). Thus, at $\omega = 2\pi \cdot 10^4$, the terms are sufficient if $x \ll 130$ μm.

The effect of the local potential is simply (to this level of approximation) to add the proximity term $P(\mathbf{r}, \mathbf{R}; a, \lambda)$ to the usual expression of one-dimensional cable theory. This term is independent of frequency and membrane capacitance although dependent on the electrode positions, fiber radius, and membrane and internal resistance. If one were quite confident that the fiber had circular cross section, and if one knew precisely the location of the microelectrodes, one could predict the size of the term. Our lack of such confidence suggests that the parameter $P(\mathbf{r}, \mathbf{R}; a, \lambda)$ be considered as just another circuit element in the circuit model. While the physical significance of the parameter is somewhat unusual (it can, for instance, be negative even though it describes a strictly passive resistive process), mathematically it enters the equations just like any other circuit parameter. One can then determine the parameter $P(\mathbf{r}, \mathbf{R}; a, \lambda)$ with the same curve-fitting procedures (see below) used to determine the value of the other circuit parameters, for instance, membrane capacitance. The addition of this extra unknown parameter adds uncertainty to the analysis since it provides another "degree of freedom."

The distinction between the two variables $S(\mathbf{r}, \mathbf{R})$ and $P(\mathbf{r}, \mathbf{R}; a, \lambda)$ requires further discussion. Eq. 1, which includes the variable S, is the precise and general form. It shows that the total potential can be written as the sum of two terms: $L(x \cdots)$ and $S(\mathbf{r}, \mathbf{R})$. It is important to realize that *both* terms vary with longitudinal position. The term S is large and varies steeply when the longitudinal electrode separation x is small but is almost zero if x is larger than two fiber radii. For this reason one would expect there to be no significant circumferential or radial gradients of potential when the electrode separation is greater than a fiber diameter. The term L varies gradually if x is small compared to λ, but it accounts for almost the entire

decrement of potential for large x. The additional variable P is defined so we can easily analyze the variation of potential for the case in which both L and S are significant. Thus, the variable P includes the effect of both one-dimensional and three-dimensional decrement.

THEORY

Electrical Models of a Sarcomere

The circuit models which have been proposed to describe skeletal muscle fibers are, for the most part, models of the shunt admittance of a sarcomere $\mathbf{y}$ through which current flows from the sarcoplasm to the external solution. The circuits have no explicit role for the sarcoplasmic reticulum, on the assumption that, at least in the resting state, no significant current flows from the sarcoplasm through the sarcoplasmic reticulum into the tubular system and out of the muscle fiber (Leung, 1973; Ebashi and Endo, 1968; and Franzini-Armstrong, 1970, 1971). These circuit models assume the sarcoplasmic impedance to be resistive because of the paucity of contrary experimental data (Schneider, 1970; Mobley et al., 1973).

We will now discuss several circuit models of a sarcomere and present some families of curves which illustrate the expected behavior of a fiber with these properties. In all the circuit models the surface membrane is represented as a parallel combination of a resistance and capacitance. The evidence that this is an adequate representation is incomplete but measurements on artificial membranes (Hanai et al., 1964), on squid axon at frequencies below 20 kHz (Palti and Adelman, 1969), and on glycerol-treated muscle fibers (Valdiosera et al., 1974 *b*) support the assumption. The total shunt admittance is then

$$\mathbf{y} = \mathbf{y}_T + g_m + \mathbf{j}\omega c_m, \tag{5}$$

where $\mathbf{j} = \sqrt{-1}$ and ω is the angular frequency, 2π times the frequency in hertz. The variables are defined for a unit length of muscle fiber (Table I). Circuit models including a statistical distribution of circuit parameters (as described in Appendix D of Falk and Fatt, 1964) are not used here since the choice of the probability density function for each of the circuit parameters seems arbitrary and not subject to experimental test.

Lumped Model of the Tubular System

The lumped model of the tubular system, appealing because of its simplicity, has received considerable attention (Falk and Fatt, 1964; Freygang et al., 1967; Hodgkin and Nakajima, 1972 *a*; 1972 *b*; see Eisenberg, 1971; Jack et al., 1973; Peachey and Adrian, 1973, for reviews). In this model the tubular system is represented as a resistor in series with a capacitor. That is to say,

TABLE I

SETS OF VARIABLES

Electrical property	Structure itself	Surface of fictitious unfolded cylinder	Length of fiber	Volume of fiber	Dimensionless variables for curve fitting
Tubular membrane capacitance	C_w (F/cm^2)	C_w^* (F/cm^2) (often C_e)	c_w (F/cm) (often c_e)	$\bar{C}_w$ (F/cm^3)	*cec*
Tubular membrane conductance	G_w (mho/cm^2)	G_w^* (mho/cm^2)	g_w (mho/cm)	$\bar{G}_w$ (mho/cm^3)	*gwg*
Tubular luminal resistance or conductance	— G_L (mho/cm)	R_L^* (ohm-cm^2) —	r_L (ohm-cm) —	$\bar{R}_L$ (ohm-cm) $\bar{G}_L$ (mho/cm)	*rer* —
Access resistance	R_a (ohm-cm^2) (often R_e)	R_a^* (ohm-cm^2)	r_a (ohm-cm) (often r_e)	—	*rare*
Surface membrane resistance or conductance	R_m (ohm-cm^2) G_m (mho/cm^2)	R_m^* (mho/cm^2) G_m^* (mho/cm^2)	r_m (ohm-cm) g_m (mho/cm)	— —	1—*rer* —
Surface membrane capacitance	C_m (F/cm^2)	C_m^* (F/cm^2)	c_m (F/cm)	—	1—*cec*
Sarcoplasmic resistivity	R_i (ohm-cm)	—	r_i (ohm/cm)	R_i (ohm-cm)	—

Most authors do not explicitly distinguish between the starred and unstarred variables since detailed information concerning the shape and folding of muscle fibers is not available. The variables referred to the volume of fiber and to the structure itself are defined and related in Adrian, Chandler, and Hodgkin (1969). The variables referred to the surface of a fictitious unfolded cylinder are used by Falk and Fatt (1964) and Freygang et al. (1967); the relations of these variables to those of a unit length of muscle fiber are discussed in those references and in Hodgkin and Rushton (1946) and Jack et al. (1973). The dimensionless variables are defined in this paper.

all the resistance of the tubular system is supposed to arise at one place, most likely the mouth of the tubules and this resistance is assumed to be in series with the total capacitance of all the tubular membranes. Thus, we can write (again using the variables defined in Table I)

$$\mathbf{y}_T = \frac{1}{r_a - \mathbf{j}\,\frac{1}{\omega c_w}}. \tag{6}$$

Reference to Fig. 1 will show that this model is distinguished by the absence of a circuit element to represent the resistance of the solution in the lumen of the tubules. The lumped model then predicts that there should be no radial gradients of potential within the tubular system in disagreement with the straightforward interpretation of the experimental results of González-Serratos, 1971; Adrian, Costantin, and Peachey, 1969; Costantin, 1970; and Hodgkin and Nakajima 1972 *a*, 1972 *b*.

The lumped model does not explicitly include the resistance of the membrane of the tubules because it cannot be identified by electrical measurements made at one location, just as two resistors in parallel cannot be distinguished from an equivalent single resistor (Eisenberg, 1965; Eisenberg, 1967; Schneider, 1970).

In order to predict the impedance of the lumped model it is necessary to consider the particular form of the appropriate equations. Difficulties arise if the circuit parameters are not normalized because changes in one parameter have complicated effects on the whole curve even at low frequencies. We describe the lumped model by the "normalized" variables $\underline{r}$, $\underline{c}$, *rer*, and *cec*. Note that we follow the convention of computer languages and allow variables to be named by more than one letter; multiplication is indicated explicitly.

The variable $\underline{r}$ is the DC resistance of the membranes in a unit length of muscle fiber.

c_m is the capacitance of the surface membrane in a unit length of muscle fiber.

c_w is the capacitance of the tubular wall in a unit length of muscle fiber.

$\underline{c}$ is the sum of the capacitance of the surface membrane and of the membrane of the tubular system in a unit length of muscle fiber, $\underline{c} = c_w + c_m$. Note that $\underline{r} \times \underline{c}$ is a measure of the overall "time constant" of the muscle fiber.

cec is the ratio of the capacitance of the tubular system to the capacitance c, both measured in a unit length of muscle fiber, $cec = c_w/\underline{c}$.

rer is the ratio of the resistance at the mouth of the tubules r_a to the DC resistance, both measured in a unit length of muscle fiber $rer = r_a/\underline{r}$.

These are related to the variables used by Falk and Fatt and Freygang et al. (1967) by the following equations:

$$c_w = c_e; \quad r_a = r_e; \quad \underline{c} = c_m + c_e; \quad \underline{r} = r_m;$$

$$cec = \frac{c_e}{c_e + c_m}; \quad rer = \frac{r_e}{r_m}, \tag{7}$$

where the variables on the right hand side of the equations are defined by those authors. We can now generate plots of the phase angle between sinusoidal current and voltage expected for various circuit parameters using Eqs. 1, 3, 5, and 6 to generate the impedance, and then determining the phase angle of the voltage.

Figs. 3 and 4 show the effect of the variation in the parameters *rer* and *cec*, the other variables being held constant at the values indicated in the captions. The effects of the proximity parameter are quite similar to those illustrated in Fig. 7 for another circuit model. In the other figures $P(\mathbf{r}, \mathbf{R}; a, \lambda)$ is unrealistically set to zero in order to facilitate comparisons with previously published

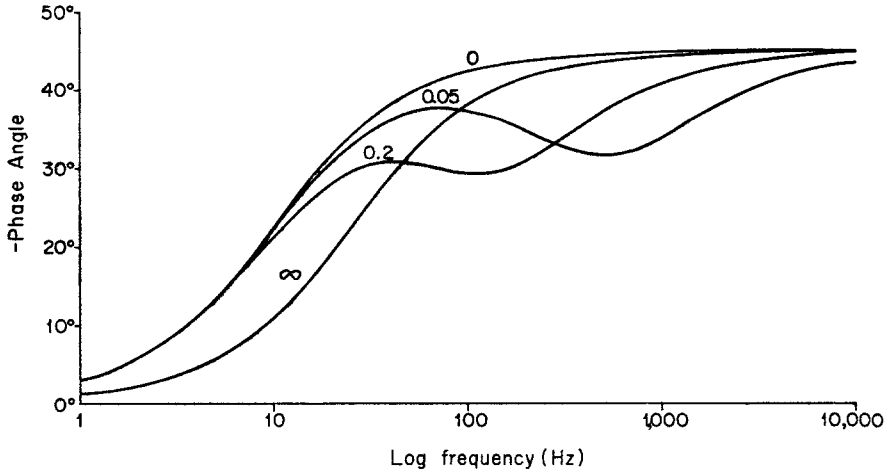

FIGURE 3. The effects of *rer*, the ratio of radial to "membrane" resistance, on the phase characteristic of the lumped model. The values of *rer* are indicated. The other variables were held constant at the values *cec* = 0.6, $P = 0$, and $\tau \times \varsigma = 0.0162$ s.

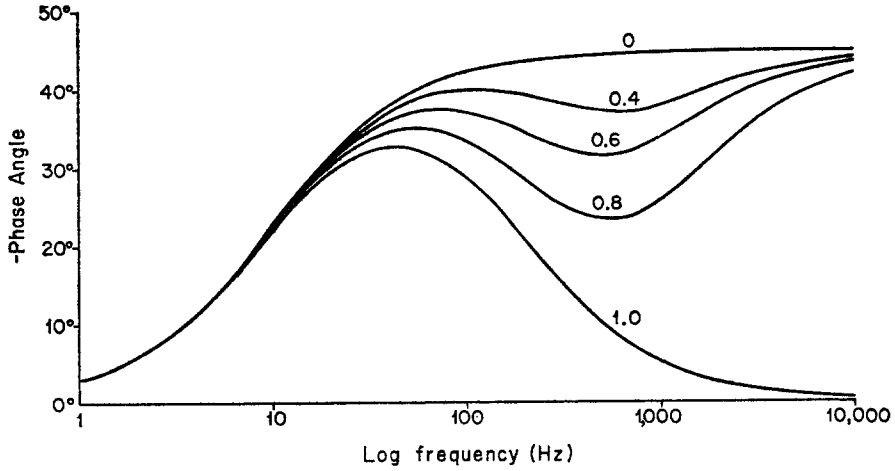

FIGURE 4. The effect of *cec*, the ratio of tubular to total capacitance, on the phase characteristic of the lumped model. The values of *cec* are indicated. The other variables were held constant at the values *rer* = 0.05, $P = 0$, $\tau \times \varsigma = 0.0162$ s.

curves. The effects of τ and ς are not shown since the phase plot depends in a simple way on the product of τ and ς; these variables simply translate the plot left and right. The dependence on the variable *rer*, which specifies the radial resistance to current flow, is as one might expect. If *rer* = 0, the resistance r_a at the mouth of the tubules is zero and the equivalent circuit of a sarcomere is just a resistance in parallel with the capacitance ς. The phase plot is then the arctangent function shown. Similarly, if *rer* is infinite, the capacitance of the

tubular system is electrically isolated from the rest of the admittance y_T and the equivalent circuit is just a resistor and capacitor c_w in parallel, and the phase plot is the arctangent function. Between the extremes, the main effects of *rer* are to change the frequency at which the minimum in the phase plot occurs and to change the height of the low frequency maximum.

The effect of the variable *cec* which specifies the fraction of total capacitance on the tubular system, is shown in Fig. 4. When *cec* = 0, there is no capacitance in the tubular system and the curve is a simple arctangent function. When *cec* = 1, there is no capacitance on the surface membrane; all the capacitance in the fiber is in series with resistance, and the phase plot must then approach zero at high frequencies. Between these extremes, the main effect of *cec* is to change the height of the maximum and the depth of the minimum of the plase plot. The variable *cec* has little effect on the frequency at which these extrema occur.

Hybrid Model of the Tubular System

It seems likely that the resistance of the lumen of the tubules has a significant effect on the electrical properties of muscle fibers and so it is important to include such a resistance in the circuit model of a sarcomere. Peachey and Adrian (1973) have introduced such a model including both the luminal resistance of the tubules and an "access resistance" at the mouth of the tubules (see also Peachey, 1973). We shall refer to this model as the "hybrid" model so as not to prejudge the physical location of the access resistance.

In order to describe this model we use the dimensional variables

r_m = the DC resistance of the surface membrane in a unit length of muscle fiber, equal to $R_m^*/2\pi a$;

g_w = the DC conductance of the tubular membranes in a unit length of muscle fiber, equaling $\bar{G}_w \pi a^2$;

c_w = the total capacitance in the tubular membranes in a unit length of muscle fiber, equaling $\bar{C}_w \pi a^2$;

c_m = the capacitance in the surface membrane of a unit length of muscle fiber, equaling $C_m^* 2\pi a$;

r_a = the access resistance in a unit length of muscle fiber, equaling $R_a^*/2\pi a$;

r_L = the radial resistance of the lumen of the tubules in a unit length of muscle fiber, is defined as $1/8\pi \bar{G}_L$ so the low frequency behavior of a hybrid model with total radial resistance r_L is similar to the low frequency behavior of the lumped model with radial resistance $r_a = r_L$ (Adrian, Chandler, and Hodgkin, 1969, Eq. 14). The variables undefined here are discussed in Table I, in Adrian, Chandler, and Hodgkin (1969), and in Peachey and Adrian (1973). The radius of the hypothetical right circular cylindrical muscle fiber used in the calculation of the starred variables is taken as a centimeter.

The normalized variables which seem most helpful (out of many possible choices) in generating families of phase plots are

$\underline{c} = c_m + c_w$ is the total capacitance of the tubular and surface membranes in a unit length of muscle fiber

$cec = c_w/c$

$\underline{r} = [1/r_m + 1/(r_a + r_L + 1/g_w)]^{-1}$ is approximately equal to the DC resistance to the current flowing out of a unit length of muscle fiber; it would be equal to this resistance if the length constant of the tubular system were much larger than the radius of the muscle fiber (see Eq. 14 of Adrian, Chandler, and Hodgkin, 1969). This variable must be distinguished from r_m, the resistance of the surface membranes in a unit length of muscle fiber.

$rer = r_a + r_L/\underline{r}$;

$gwg = \underline{r} \times g_w$;

$rare = r_a/(r_a + r_L)$.

The equation which describes the admittance of the tubular system in this model is a generalization of Eq. 14 of Peachey and Adrian (1973), the generalization to the sinusoidal case being made by the techniques described by Eisenberg and Engel (1970), Appendix 2. The generalization essentially replaces each membrane resistance with the corresponding membrane impedance and interprets the resulting complex quantity as the impedance defined by Laplace transform theory

$$\frac{1}{\mathbf{y}_T} = \frac{4r_L}{\boldsymbol{\Gamma} a}\frac{I_0(\boldsymbol{\Gamma} a)}{I_1(\boldsymbol{\Gamma} a)} + r_a, \tag{8}$$

where $\boldsymbol{\Gamma}$, a function of frequency, is the appropriate generalization of the length constant of the tubular system:

$$\boldsymbol{\Gamma} = \frac{2}{a}(2g_w r_L)^{1/2}(1 + \mathbf{j}\omega c_w/g_w)^{1/2}, \tag{9}$$

and $I_0(\mathbf{z})$, $I_1(\mathbf{z})$ are modified Bessel functions of the first kind (Watson, 1944). In order to study the phase characteristics of the hybrid circuit model, Eqs. 8 and 9 are written in terms of the normalized variables defined above and then substituted into Eqs. 5 and 3.

Actual calculation of the phase characteristics described by 8 and 9 requires the generation of complex Bessel functions for many complex arguments. The calculation is tedious to perform by hand and so we have used the interactive computing language APL/360 (Gilman and Rose, 1970) in the APL*PLUS implementation (Scientific Time Sharing, 1971). A most efficient method of generating Bessel functions for real arguments is to use rational approximations (Hart et al., 1968) but the validity of these approxi-

mations has not been studied in the complex domain. We therefore generate the Bessel functions by the appropriate asymptotic expansion when the magnitude of the argument is large, and by the defining Taylor series when the magnitude of the argument is small (Watson, 1944). Sufficient terms were taken to guarantee accuracy of four significant figures in all cases. The routines used were extensively checked against tables of Bessel functions of real arguments and the appropriate Kelvin functions (Abramowitz and Stegun, 1964) and against tables of the Bessel functions of complex argument. It should be noted that the only table of Bessel functions of complex argument available to us (National Bureau of Standards, 1947) uses a convention in its choice of the location of the zero phase line of $I_0(\mathbf{z})$ which differs from that used by Watson (1944, p. 77) and most other authors.

Figs. 5–7 show phase characteristics of the hybrid model, computed for parameters close to those of muscle fibers in normal Ringer. In Figs. 5, 6 the three-dimensional parameter is set to zero. The effects of the variables $\underline{r}$ and $\underline{c}$ are to shift the characteristic left and right. Similarly, the effects of *rer*, the radial resistance variable, are qualitatively similar (although less marked and occurring at higher frequencies) to the effects in the lumped model (see Fig. 3). Fig. 5 shows the plots produced by variation of *cec*, the variable which determines the capacitance of the tubular system. Again *cec* changes the depth of the minimum and the height of the maximum, but the effects here are less dramatic than in the lumped model. The difference between the models is particularly striking for large values of *cec*. In the hybrid model

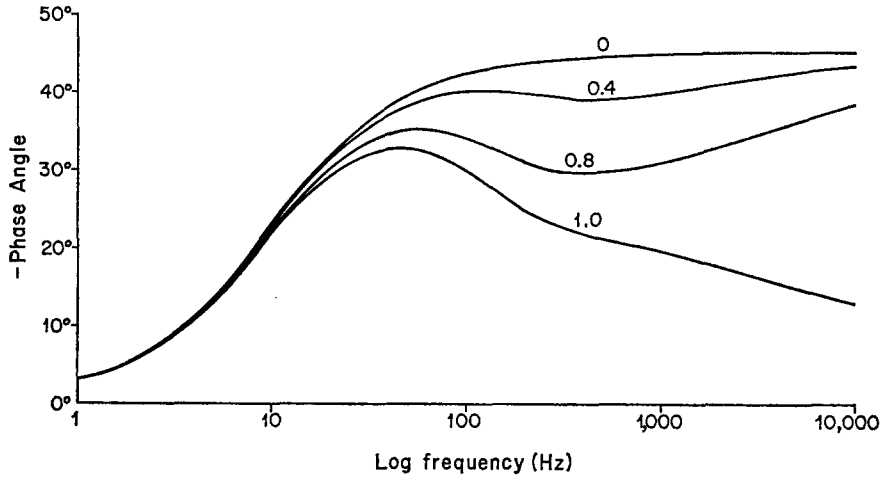

FIGURE 5. The effect of *cec*, the ratio of tubular to total capacitance, on the phase characteristic of the hybrid model. The values of *cec* are indicated. The other variables were held constant at the values *rer* = 0.05, $P = 0$, $\underline{r} \times \underline{c} = 0.0162$ s, *rare* = 0.15, *gwg* = 0.182. The values of the variables are taken from the Valdiosera et al. (1974 *b*), except that *gwg* is determined from the data of Eisenberg and Gage (1969).

cec = 1 again implies that all the capacitance of the fiber is in the tubular system, and so all the capacitance is in series with the resistance r_a, but now this resistance is a much smaller value and so the decrease in phase with frequency is more gradual and occurs at higher frequencies.

The effect of *gwg*, the variable which measures the conductance of the tubular wall is not shown because the phase plot is hardly changed by this variable. This property is to be expected (Schneider, 1970: Fig. 14) since for these sets of circuit parameters at low frequencies there is little decrement of potential in the tubular system, and the hybrid model behaves like the lumped model (see indented text on p. 441). At higher frequencies, where there is significant decrement in the tubular system, the conductance of the tubular membranes is not very important compared to their capacitance. Since *gwg* has a small effect on any of the passive electrical properties of the muscle fiber, it cannot be determined from electrical measurements under one set of conditions. On the other hand, incorrect estimates of the value of *gwg* will have a negligible effect on the estimates of the other parameters which describe the linear electrical properties of the muscle fiber.

Fig. 6 shows the effect of *rare*, the variable which specifies the location of the resistance to radial current flow. When *rare* = 1, the hybrid model and the lumped model are identical and indeed we have used this property as an overall check on our calculations. In this case the depth of the minimum in the curve is quite large. If *rare* = 0, all the radial resistance of the tubular system is supposed to arise in the lumen of the tubules, and the depth of the minimum is quite shallow.

Fig. 7 shows the three-dimensional variation in potential, and in phase angle, in some detail since similar curves have not previously been published.

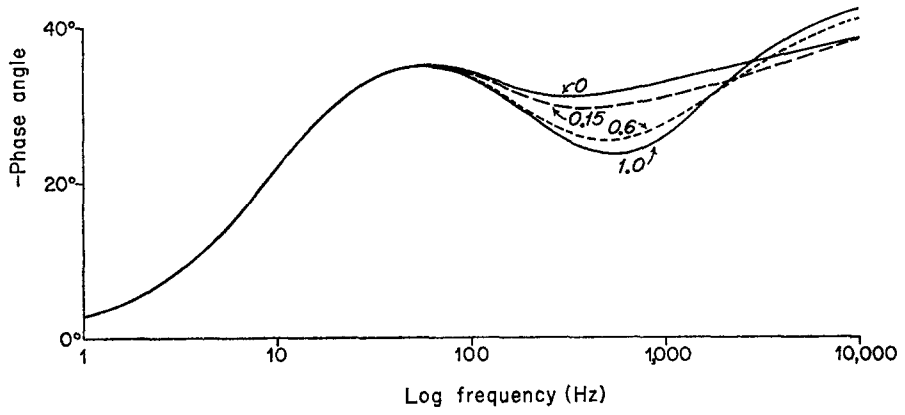

FIGURE 6. The effect of *rare*, the variable which specifies the location of the radial resistance, on the phase characteristic of the hybrid model. The values of *rare* are indicated. The other variables were held constant at the values *rer* = 0.05, $P = 0$, $\underline{r} \times \underline{c} = 0.0162$ s, *cec* = 0.8, *gwg* = 0.182.

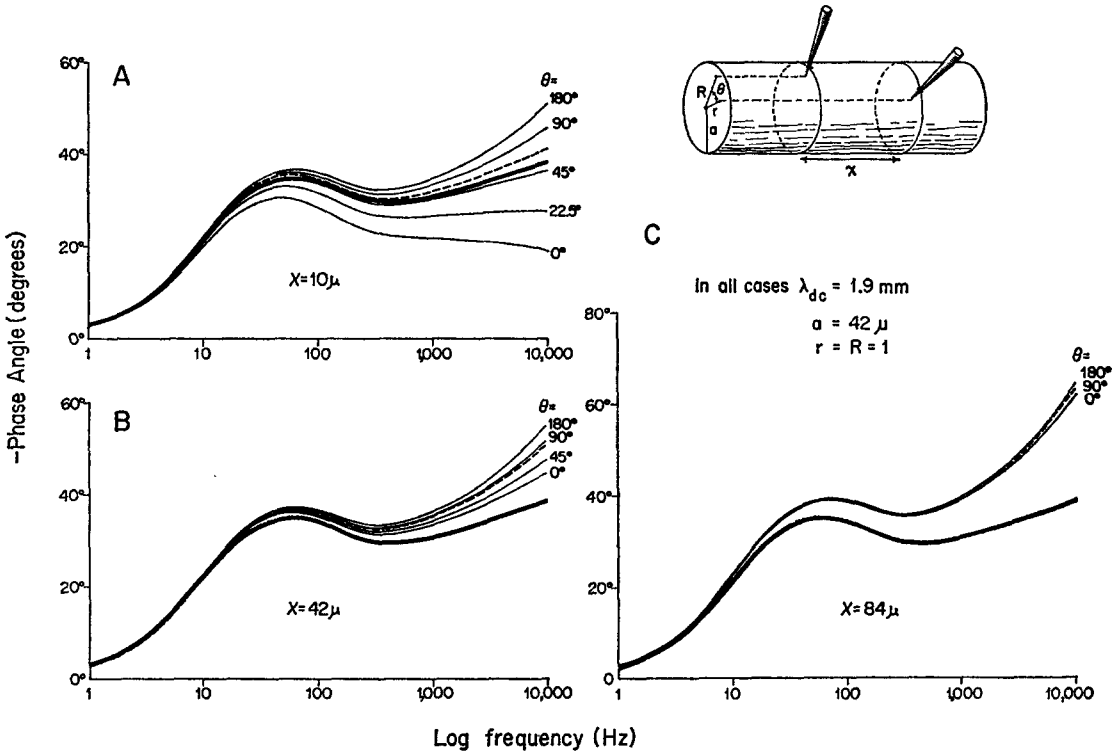

FIGURE 7. The circumferential variation in potential expected at various microelectrode positions. The insert shows the coordinate system used throughout the paper: the circumferential coordinate is θ; the radial coordinate is r; the longitudinal coordinate x; the fiber radius is a. The heavy solid curve is the phase characteristic determined when $P = 0$, that is when there is no increment or decrement in potential produced by the one- or three-dimensional flow of current. This heavy curve is that predicted by one-dimensional cable theory at $x = 0$. The heavy dashed curve is that predicted by one-dimensional cable theory at the longitudinal separation shown. The thin curves are the phase characteristics predicted by three-dimensional theory. Notice that the curves in A are qualitatively similar to those shown in Fig. 2. Only in C, where the separation is one fiber diameter, does the circumferential variation of phase angle become negligible, but in this case the effect of one-dimensional decrement is large. The values of the circuit parameters were $\underline{r} \times \underline{c}$ = 16.2 ms; *rer* = 0.05; *cec* = 0.8; *gwg* = 0.182; *rare* = 0.15; λ = 1.86 mm; a = 42 μm; the three-dimensional correction was determined from Table 3 of Eisenberg and Johnson (1970) for the case where both electrodes are just under the surface membrane. (In figure μ = μm.)

The calculations were made from Eqs. 1, 8, and 9 using the values of $S(\mathbf{r}, \mathbf{R})$ given by Eisenberg and Johnson (1970) for microelectrodes located just under the surface membrane. The size of the correction is influenced by the depth of the microelectrodes but not sufficiently to change the implications of the figure. Fig. 7 A is similar to the experimental results shown in Fig. 2. Fig. 7 B is computed at the electrode separation recommended by Falk and

Fatt (1964), Eisenberg (1967), and Eisenberg and Johnson (1970). It can be seen that at this electrode separation the circumferential variation of phase is reduced but not negligible. While it might in principle be possible to find some locations in a right circular cylindrical fiber at which $P = 0$ and there were no three-dimensional effects, it would be difficult to place microelectrodes in that location since methods to observe and control the radial position of microelectrodes have not been worked out.

Fig. 7 C shows the phase characteristic at an electrode separation (a fiber diameter) at which the circumferential variation of potential is unimportant. This figure is reminiscent of the results of Freygang and Trautwein (1970) on the impedance of cardiac muscle. At these electrode locations it is possible to neglect the variation of P and membrane potential with circumferential and radial position: P varies significantly only with x, see Eq. 4. It may seem that measurements made at this or larger electrode separations would avoid three-dimensional effects and so would be simpler to interpret than measurements at smaller electrode separations. This is not the case, however, since P is important at large separations because of its one-dimensional component $-x/\lambda$ (see Eq. 4) and must be taken into account when computing the impedance or phase characteristics.

Disk or "Distributed" Model of the Tubular System

This model attempts to describe the tubular system as a disk of membrane with a resistive interior. The only resistance to radial current flow is in the lumen of the tubules. The disk model was introduced by Falk and Fatt (1964) and modified and elucidated by Adrian, Chandler, and Hodgkin (1969) and Schneider (1970). It has been extensively used (Hodgkin and Nakajima, 1972 *a*, 1972 *b*; Adrian, Constantin, and Peachey, 1969; Costantin, 1970, among others) since it seems a plausible representation of the electrical properties of the tubular system.

While historically the hybrid model arose as an extension and generalization of the disk model, it is more convenient here to view the disk model as a special case of the hybrid model, with the variable *rare* constrained to zero (Fig. 6). The effects of the variables τ, ς, *rer*, and *gwg* are as described above. The effect of the variable *cec*, the variable which specifies the capacitance of the tubular system, is different, however, (Fig. 8). At low values *cec* sets the minimum in the phase plot; at higher values however, there is no longer a minimum at all. Indeed for *cec* = 1, in which case all the capacitance of the muscle fiber is in the tubular system, the curve approaches 22.5° at high frequencies. This is to be expected (Falk and Fatt, 1964) since at such high frequencies the tubular system behaves as one distributed network distributed along another network. Each network is in itself described by a square root function and so the overall phase shift at high frequencies is $(\frac{1}{2}) \times (\frac{1}{2}) \times$

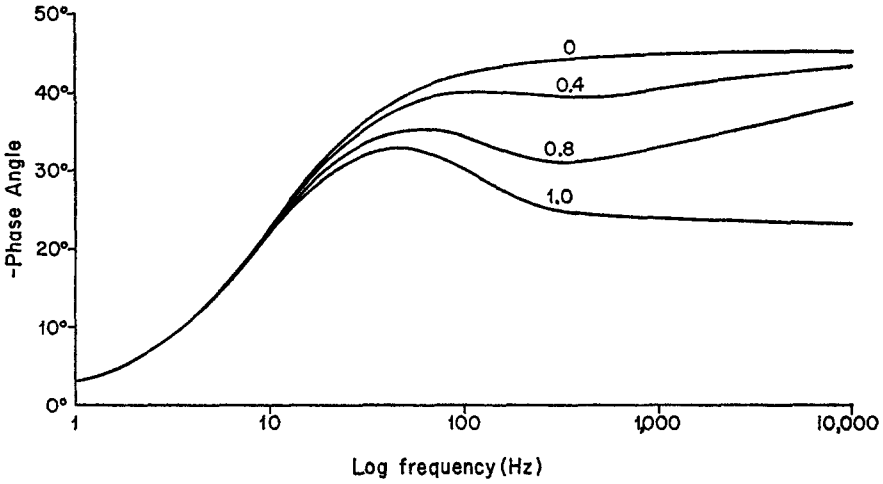

FIGURE 8. The effect of *cec*, the ratio of tubular to total capacitance, on the phase characteristic of the disk model. The value of *cec* is indicated. The other variables were held constant at the values *rer* = 0.05, *gwg* = 0.182, $\underline{r} \times \underline{c}$ = 0.0162 ms, P = 0 and, because we are dealing with the disk model, *rare* = 0. Note the limiting value at high frequencies in the case of *cec* = 1.

(−90°). The properties of the phase characteristic when *cec* = 0 and when *cec* = 1 serve to check our calculations.

Determination of Circuit Parameters

The passive electrical properties of muscle fibers can be determined by fitting one of the circuit models described above to the impedance data recorded experimentally from a muscle fiber. The procedure of fitting the data should satisfy several criteria. The results of the procedure should depend on the experimental data at all frequencies, emphasizing the midfrequency data which is usually most accurate. The procedure should provide an objective, statistically defined measure of fit and the standard deviation of the estimates of the circuit parameters. (This will amount to a measure of how sensitive the theoretical phase characteristic is to each of the circuit parameters). It should provide an indication of the correlation coefficient between the circuit parameters so that one can determine if two circuit parameters are closely correlated and cannot be evaluated independently. It should be possible to determine the best fit with any of the variables constrained to a particular value. Finally, the procedure should be convenient and not too expensive in computer time, since a large number of curve fits will certainly be necessary in the analysis of experimental results.

We have used the curve-fitting method derived and analyzed by Hamilton (1964, 1965) for the determination of molecular structures from crystallo-

graphic data and are indebted to Professor David Eisenberg for bringing this work to our attention.

A discussion of the curve-fitting method requires the definition of the following variables. Precise definition is necessary here since different authors use different notations for the same quantities. $\Phi_i(\omega_i)$ is the phase angle experimentally observed at the known angular frequency ω_i. The index $i = 1, 2, 3, \cdots M$ where M is the number of frequencies at which data is recorded. $\theta_i(\omega_i ; \beta_j)$ is the phase angle theoretically predicted at the angular frequency ω_i for the values of the circuit parameters β_j. Each β_j is a different parameter and $j = 1, 2, 3, \cdots N$ where N = number of independent circuit parameters whose values we wish to determine. The procedure to determine the best values of the circuit parameters β_j and their variance depends on the distribution of the experimental data. The recommended procedure (Hamilton, 1965, Chap. 4, 5) for data with a Gaussian distribution is to seek the values of β_j which minimize the mean square error between the theoretically predicted and experimentally observed phase angles.[3] The function minimized is:

$$\psi = \sum_{i=1}^{M} w_i F_i^2(\Phi_i ; \theta_i), \tag{10}$$

where the weights w_i are defined and discussed below and

$$F_i(\Phi_i ; \theta_i) = \Phi_i(\omega_i) - \theta_i(\omega_i ; \beta_j). \tag{11}$$

There are a number of methods for finding the minimum of the function ψ. We have used the Levenberg-Marquardt algorithm (Marquardt, 1963) as implemented by Brown (Brown and Dennis, 1972) because it is convenient, efficient, and converges quite well.

The choice of the weights w_i (which are positive numbers between zero and one) depends on the particular situation. If we fit the data from one muscle fiber, we set the weights to unity, although at times lower values are chosen for points contaminated by systematic error. If we fit the data from many muscle fibers in the same solution, the phase Φ_i is taken as the mean of the data from all the fibers at that frequency and the weight is chosen as the square of the reciprocal of the standard error of the mean of Φ_i (Hamilton, 1964, p. 146–149) although again lower values are chosen if the data is contaminated by systematic error. The standard deviation of the parameters

[3] The distribution of our phase data is almost Gaussian. We have constructed standardized histograms of experimental phase data at each frequency and then have standardized the sum of these histograms to form a final histogram of our measurements (2,640 observations from 98 muscle fibers in 7 solutions). This procedure has been adopted to remove from the final histogram the dependence of phase angle on frequency. The final histogram is fit surprisingly well by a Gaussian distribution.

(the square root of the variance) is computed from the following formula

$$var\ \beta_j = \frac{\sum_{i=1}^{M} w_i F_i^2}{(M - N) \sum_{i=1}^{M} w_i \left(\frac{\partial F_i}{\partial \beta_j}\right)^2}, \tag{12}$$

where the value of the derivatives are estimated from their finite difference approximations. The standard deviation of each parameter is seen to be the reciprocal of the derivative of the theory curve (in the mean square sense) with respect to the parameter. Thus, if the curve significantly changes shape for changes in the value of the parameter, the derivative is large and the standard error of the parameter is small. If the curve does not change shape significantly for changes in the parameter (for instance, if the parameter were *gwg* of the hybrid model), the derivative is small and the standard deviation is large. The correlation coefficient of the parameters is computed as described by Hamilton (1964, p. 129–132).

An objective measure of fit is Hamilton's R test (a form of the F ratio test used in the analysis of variance), with

$$R^2 = \frac{\sum_{i=1}^{M} w_i F_i^2}{\sum_{i=1}^{M} w_i \Phi_i^2}. \tag{13}$$

The value of R can be looked on as a dimensionless measure of fit. Thus, a value of $R = 0.01$ would imply that theory and experiment fit within 1%. The distribution of the random variable R has been studied and so tables are available (Hamilton, 1965) which allow one to determine whether two values of R, and thus two theoretical curves, are significantly different.

The R test takes into account the number of adjustable parameters in the model used to generate the theoretical curves. If one of the models has more adjustable parameters than the other model, it must fit much better (have a much smaller value of R) if the difference between models is to be significant.

Reliability of Circuit Values

There are two ways to evaluate statistically the significance of the value of a parameter. The obvious method is to use the mean value and standard deviation of the parameter in Student's t-test. This method allows the comparison of two values of a parameter, assuming all other parameters are held constant. There is another more severe statistical method to compare two values of a parameter. In this method the best fit of the theory is determined twice, in each fit the parameter is constrained to one of the two values being compared. Comparison of the goodness of fit (the value of R) in the two cases allows

determination of the significance of the difference between the two values of the parameter. This test has the important advantage that the values of all the other parameters are free to take on their best values.

It should be clearly recognized, however, that the important conclusions concerning goodness of fit and the significance of parameter values must be made on the basis of human judgment. The statistical theory does not include the effects of covariance of experimental observations, covariance of theoretical variables, or indeed the nonlinearity of the equations describing the circuit model. It cannot include the effects of unknown systematic errors. The statistical theory then can serve to reject hypotheses: it can clearly show that two models or two values of a parameter do *not* differ in their ability to fit data. However, the decision that two parameter values, or the fit of two models, *are* significantly different must be taken by the investigator, with due weight to all sources of uncertainty, known and yet unknown.

The most serious difficulty concerning the reliability of the estimates of the circuit parameters is not clearly shown by the above statistical discussion. Fig. 9 illustrates the problem. The synthetic "data" plotted was generated from the hybrid model. The theoretical curves shown are the best fits of the

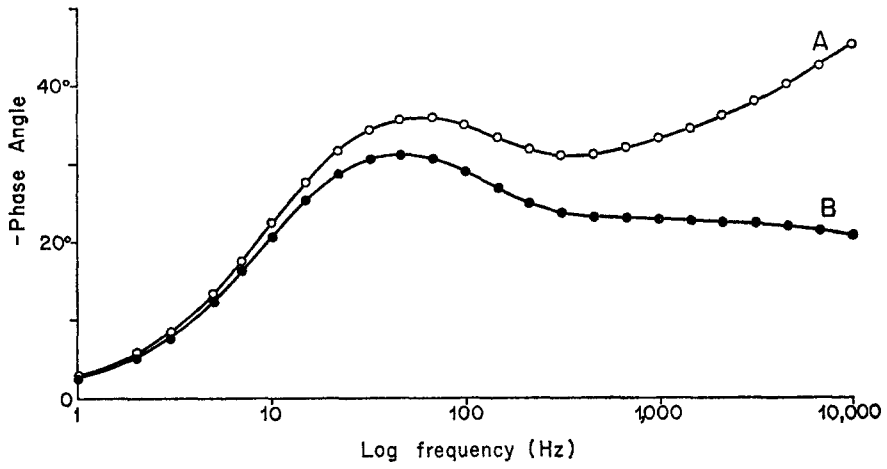

FIGURE 9. Fits to synthetic data. The data shown were generated by the hybrid model for the parameter values $\underline{r} \times \underline{c}$ = 16.2 ms; *cec* = 0.8; *rare* = 0.15; *gwg* = 0.182; *rer* = 0.05; and in A, $P(\mathbf{r}, \mathbf{R}; a, \lambda) = -0.01$, in B, $P(\mathbf{r}, \mathbf{R}; a, \lambda) = 0.05$. The two values of P correspond to two different electrode locations as shown in Fig. 2. The data was fit by both the hybrid and disk models but the fits cannot be distinguished by eye. The best parameter values for the hybrid model were the values which generated the curve (within the rounding error of the routines used to generate the functions). The parameter values which gave the best fit of the distributed model are $\underline{r} \times \underline{c}$ = 16.0 ms; *cec* = 0.88; *rer* = 0.046; and $P(\mathbf{r}, \mathbf{R}; a, \lambda) = -0.016$ for curve A, and $P(\mathbf{r}, \mathbf{R}; a, \lambda) = 0.044$ for curve B.

disk model and the fits are quite satisfactory. The best values of the circuit parameters of the disk model are given in the caption; these are significantly different from the corresponding values of the hybrid model which generated the data. Thus, an incorrect model can fit data quite satisfactorily but with incorrect parameter values. In this case independent knowledge of the correct parameter values is needed to determine the correct circuit.

It might be conjectured that the ability of an incorrect model to fit synthetic data is peculiar to models which contain the proximity parameter P. This conjecture has been refuted by performing another mock experiment, similar to that discussed above, but in this case using data generated from the hybrid model with $P = 0$ and then fitting the data with the disk model with P constrained to zero.

DISCUSSION

Circumferential and Radial Variation of Potential

The experiments described in Fig. 2 seem to show a marked circumferential and radial variation of potential and so it is important to discuss both possible errors and implications of the experiments. The most likely source of error in the experiment is the local damage produced by the microelectrode. This damage could produce a shunt in a small region around the current electrode and so produce a circumferential variation in membrane potential and concommitantly in membrane resistance. It seems unlikely that this is a major source of error here for several reasons. The fibers showed no sign of damage, even observed at high magnification with polarizing optics, and the resting potentials were of normal magnitude and stable. Most convincingly, the low frequency measurements of phase, which are very sensitive to small changes in membrane resistance and so to membrane potential, are quite stable during the experiment. Of course, such is not always the case; indeed, Fig. 2 is the result of weeks of experimentation in which the great majority of fibers did show measurable damage and drift and so were rejected.

It is interesting to compare the size of the three-dimensional effect observed with that predicted from the theory of Eisenberg and Johnson (1970) and Peskoff et al. (1973). Assuming the fiber to be a right circular cylinder, for the sake of this crude approximation, the angular coordinate of the microelectrodes can be calculated from the observed locations and fiber "diameters." The theoretical value of the proximity parameter for that position can be determined from Eq. 4 and Fig. IV. 4-2, 3 of Eisenberg and Johnson, 1970, assuming the microelectrodes to be just under the surface membrane. Table II compares the theoretical values with those which produce the best fit to the experimental data. Since the location of the microelectrodes is not known and since the fiber is unrealistically assumed to be a circular cylinder, it is not surprising that there is not very good agreement.

TABLE II

ANALYSIS OF EXPERIMENTS ON THE THREE-DIMENSIONAL EFFECT SHOWN IN FIG. 2

	Parameter values					
	$r \times c$	*cec*	*rare*	*rer*	$P(\mathbf{r}, \mathbf{R}; a, \lambda)$ (observed)	$P(\mathbf{r}, \mathbf{R}; a, \lambda)$ (predicted)
	ms	$\times 10^{-1}$	$\times 10^{-2}$	$\times 10^{-2}$	$\times 10^{-3}$	$\times 10^{-3}$
Fiber A						
Position 1	18.8	6.77	5.65	3.62	−9.36	−5.0
	(0.3)	(0.04)	(1.60)	(0.13)	(0.19)	
Position 2	18.3	7.92	3.57	4.04	4.72	20.0
	(0.4)	(0.05)	(1.55)	(0.15)	(0.43)	
Fiber B						
Position 1	14.1	7.79	25.5	7.01	−10.7	−2.0
	(0.2)	(0.02)	(1.6)	(0.15)	(0.3)	
Position 2	16.3	8.74	14.6	5.73	48.7	40.0
	(0.3)	(0.04)	(1.5)	(0.15)	(0.9)	

The theoretical curves shown in Fig. 2 were computed with the above parameter values and $gwg = 0.182$ (Eisenberg and Gage, 1969).
The numbers in parentheses are the standard deviation of the parameters.

The experiments shown in Fig. 2 provide a most critical test of our experimental procedures and results and indeed of the theoretical models of the muscle fiber. Each theoretical curve was generated by a set of parameter values for the hybrid model, the set of parameter values which give the best fit. Since the proximity parameter $P(\mathbf{r}, \mathbf{R}; a, \lambda)$ is the only variable in the impedance equations which depends on a circumferential or radial position; it is the only variable which should be different in the two sets of best values. The best parameter values and their standard deviations are given in Table II and it can be seen that while the proximity parameter is by far the most sensitive to the circumferential position, some of the other circuit parameters vary as well.

The conclusions to be drawn from Fig. 2 are important and so the curve-fitting results have been carefully checked. Use of the R test reinforces our conclusion. Fitting the disk or lumped model to the data has no effect on our conclusions; that is to say, there is still a profound circumferential variation of some parameter values. Application of corrections for the phase shift in the tip of the microelectrode or for possible phase shift in the longitudinal impedance of the muscle fiber also does not change the circumferential variation of circuit parameters, although, of course, the absolute values of the parameters do depend somewhat on the corrections.

The variation in these parameters with circumferential position serves as an upper bound on the total error in our procedures and experiments since it

includes the effects of experimental and theoretical errors as well as imperfections in the curve-fitting procedure. There are, however, other more interesting potential sources of the variation of circuit parameters with circumferential position. If there were, for instance, a circumferential variation of potential across the tubular membranes, all the electrical models of the muscle fiber would be incorrect since they do not permit such variation. One would then expect to find a variation in the values of the circuit parameters which produce the best fit of data taken at different circumferential positions. Possible source of circumferential potential gradients across the tubular membranes are discussed below.

Any other error in the circuit models could also, at least theoretically, produce an apparent circumferential variation of parameter values. An incorrect theory might still be able to fit the data with incorrect values of the circuit parameters; and since the choice of these incorrect values would be somewhat arbitrary, they might even depend on the circumferential position of the microelectrodes. However, in the mock experiment shown in Fig. 9 the only circuit parameter which varies with position is the proximity parameter, as it should be, and so this theoretical possibility seems unlikely to be important in practice.

We conclude then that the apparent circumferential variation of circuit parameters is most likely the result of two effects: the errors in our measurements and experimental procedures and errors in the circuit models themselves, produced by circumferential variation of potential across the tubular membranes. Further experiments, in which the experimental errors are reduced to negligible values, are needed before it can be concluded that the circuit models are in error.

Approximations in the Disk Model of the Tubular System

In this section we consider several of the approximations used in the derivation of the disk model of the tubular system (Adrian, Chandler, and Hodgkin, 1969). The discussion can be immediately generalized to the hybrid model since the two models are closely related.

In the disk model the geometry of the tubular system is represented as a regular branched network of tubules, with diameter small compared to the mesh of the network. The mesh spacing is considered to be small compared to the diameter of the fiber and to the electrical length of the tubular system. The tubular system is supposed to be symmetrical and bounded by an outer membrane of circular cross section.

The precise analysis of the electrical properties of a muscle fiber would require consideration of the variation of potential within the tubular system and within the sarcoplasm of the muscle fiber. The potential across the tubular membrane has been calculated by assuming that there is no circumferential

variation of potential in the tubular lumen and that the radial variation of the potential across the tubular membranes arises entirely because of the radial variation of the potential in the tubular lumen. Mathematical difficulties force us to follow this approach and ignore the component of tubular membrane potential produced by the three-dimensional spread of potential in the sarcoplasm although we do include the current flow across the surface membrane produced by three-dimensional spread of potential.

Thus, there is an obvious source of circumferential variation of potential across the tubular membranes which the disk theory ignores: the potential in the sarcoplasm is known (Fig. 2) to vary significantly with angular location and so the potential across the tubular membrane must be expected to show such variation as well. Indeed there is experimental evidence (Adrian et al., 1969) that the local potential around a current-passing microelectrode can cause contraction, perhaps by depolarizing the nearby tubular membranes. Another obvious source of circumferential variation of potential is the irregular shape of the muscle fiber (Blinks, 1965). If current were applied to such an irregular fiber from a disk source, there would be almost no circumferential variation of potential in the sarcoplasm, but the potential in the lumen of the tubules and across the tubular membrane would still vary around the fiber. Since the disk and hybrid models do not permit circumferential variation of tubular membrane potential, it is not surprising that the values of the parameters of those models necessary to fit experimental data show a variation with circumferential position.

Another difficulty with the disk model is the assumption that the electrical length of the tubular system is much larger than the spacing of the mesh. At a frequency of 500 Hz the electrical length of the tubular system is about 10 μm in our experiments (Eisenberg et al., 1972, Eq. 11; Eisenberg, 1970, Eq. 2). Since the mesh spacing is about 1 μm (Peachey, 1965), the assumption that the electrical length is much larger than the mesh spacing will begin to fail at quite low frequencies (well below the reciprocal of the rise time of an action potential), and will be in serious error at higher frequencies. Indeed, at 10,000 Hz the electrical length of the tubular system is just 2 μm!

Hybrid Model as a Modification of the Disk Model

It is interesting to discuss the nature of the errors introduced into the disk model by the approximations just analyzed. As the electrical length of the tubular system approaches the mesh spacing one would expect deviations from the disk model for two reasons. First, the breakdown of one of the assumptions of the disk model would most likely produce deviations. Second, the structure of the tubular system is specialized just under the membrane (Peachey, 1965; Peachey and Adrian, 1973; Peachey, 1973) and this specialization should become important as the electrical length of the tubular

system becomes short. These deviations might appear as a frequency dependence of the two parameters σ and ρ (a tortuosity factor and the volume fraction of the tubular system) treated as constants by Adrian, Chandler, and Hodgkin (1969).

The hybrid model of the tubular system attempts to remedy these problems by introducing another resistance, the access resistance, into the electrical model of the tubular system. This resistance is supposed to limit the flow of current into the tubules, especially at high frequencies. The access resistance may be the property of a real structure or may represent the properties of the specialized geometry of the tubules just below the surface of the fiber.

It is important to remember, however, that the hybrid model has one more adjustable parameter than the disk model and so it should come as no surprise that it can account for the electrical properties of muscle fibers (Peachey and Adrian, 1973; Valdiosera et al., 1974 *b*) somewhat better than the disk model. The hybrid model may represent the electrical properties more satisfactorily only because it has an extra adjustable parameter which can compensate, in some subtle way, for the approximations inherent in the disk model. An evaluation of the significance of the access resistance, including its anatomical correlate, awaits further evidence, hopefully direct, concerning the radial spread of potential in the tubular system.

We are indebted to Drs. F. Rasmussen and S. Hagiwara who made it possible for us to work together. Drs. Adrian, Freygang, Mobley, Nakajima, Y. Nakajima, and Peachey kindly sent us unpublished manuscripts and made useful criticisms of the text. We particularly thank Drs. Costantin, Leung, Mobley, Peskoff, and B. Eisenberg for their illuminating discussions and searching review of the manuscripts.

The experimental work was supported by NIH grant HL 13010, the theoretical work and computation by NSF grant GB24965. Dr. Valdiosera was supported by NIH training grant GM 00448.

Note Added in Proof Mobley, Leung, and Eisenberg (*J. Gen. Physiol.*, 1974, in press) have recently shown that the longitudinal impedance of skinned muscle fibers is purely resistive.

Received for publication 30 July 1973.

REFERENCES

ABRAMOWITZ, M., and I. A. STEGUN. 1964. Handbook of Mathematical Functions. National Bureau of Standards. Washington, D. C.

ADRIAN, R. H., W. K. CHANDLER, and A. L. HODGKIN. 1969. The kinetics of mechanical activation in frog muscle. *J. Physiol.* (*Lond.*). **204**:207.

ADRIAN, R., L. L. COSTANTIN, and L. D. PEACHEY. 1969. Radial spread of contraction in frog muscle fibers. *J. Physiol.* (*Lond.*). **204**:231.

BARCILON, V., J. D. COLE, and R. S. EISENBERG. 1971. A singular perturbation analysis of induced electric fields in nerve cells. *SIAM* (*Soc. Ind. Appl. Math.*) *J. Appl. Math.* **21**:339.

BLINKS, J. R. 1965. Influence of osmotic strength on cross-section and volume of isolated muscle fibers. *J. Physiol.* (*Lond.*). **177**:42.

BOZLER, E., and K. S. COLE. 1935. Electric impedance and phase angle of muscle in rigor. *J. Cell Comp. Physiol.* **6**:229.

BROWN, K. M., and J. E. DENNIS. 1972. Derivative free analogues of the Levenberg-Marquardt and Gauss Algorithms for nonlinear least square approximation. *Numer. Math.* **18:** 289.

COSTANTIN, L. L. 1970. The role of sodium current in the radial spread of contraction in frog muscle fibers. *J. Gen. Physiol.* **55:**703.

DESOER, C. A., and E. S. KUH. 1969. Basic Circuit Theory. McGraw-Hill Book Company New York. 876 pp.

EBASHI, S., and M. ENDO. 1968. Calcium ion and muscle contraction. *Prog. Biophys. Mol. Biol.* **18:**125.

EISENBERG, R. S. 1965. A. C. Impedance of single muscle fibres. Ph.D. Thesis, University of London.

EISENBERG, R. S. 1967. Equivalent circuit of crab muscle fibers as determined by impedance measurements with intracellular electrodes. *J. Gen. Physiol.* **50:**1785.

EISENBERG, R. S. 1971. The equivalent circuit of frog skeletal muscle fibers. *In* Contractility of Muscle Cells and Related Processes R. J. Podolsky, editor. Prentice-Hall, Inc. Englewood Cliffs, N. J. 73.

EISENBERG, R. S., and E. ENGEL. 1970. The spatial variation of membrane potential near a small source of current in a spherical cell. *J. Gen. Physiol.* **55:**736.

EISENBERG, R. S., and P. W. GAGE. 1969. Ionic conductance of the surface and transverse tubular membranes of frog sartorius fibers. *J. Gen. Physiol.* **53:**279.

EISENBERG, R. S., and E. A. JOHNSON. 1970. Three dimensional electric field problems in physiology. *Prog. Biophys. Mol. Biol.* **20:**1.

EISENBERG, R. S., P. C. VAUGHAN, and J. N. HOWELL. 1972. A theoretical analysis of the capacitance of muscle fibers using a distributed model of the tubular system. *J. Gen. Physiol.* **59:**360.

FALK, G., and P. FATT. 1964. Linear electrical properties of striated muscle fibers observed with intracellular electrodes. *Proc. R. Soc. Lond. B Biol. Sci.* **160:**69.

FRANZINI-ARMSTRONG, C. 1970. Studies of the triad. I. Structure of the junction in frog twitch fibers. *J. Cell Biol.* **47:**488.

FRANZINI-ARMSTRONG, C. 1971. Studies of the triad. II. Penetration of tracers into the junctional gap. *J. Cell Biol.* **49:**196.

FREYGANG, W. H., JR., S. I. RAPOPORT, and L. D. PEACHEY. 1967. Some relations between changes in the linear electrical properties of striated muscle fiber and changes in ultrastructure. *J. Gen. Physiol.* **50:**2437.

FREYGANG, W. H., and W. TRAUTWEIN. 1970. The structural implications of the linear electrical properties of cardiac Purkinje strands. *J. Gen. Physiol.* **55:**524.

GILMAN, L. and A. J. ROSE. 1970. APL/360: An Interactive Approach. John Wiley & Sons, Inc. New York.

GONZÁLEZ-SERRATOS, H. 1971. Inward spread of activation in vertebrate muscle fibers. *J. Physiol. (Lond.).* **212:**777.

HAMILTON, W. C. 1964. Statistics in Physical Science. The Ronald Press Company New York.

HAMILTON, W. C. 1965. Significance tests on the crystallographic R factor. *Acta Crystallogr. Sect. B.* **18:**502.

HANAI, T., D. A. HAYDON, and J. TAYLOR. 1964. An investigation by electrical methods of lecithin-in-hydrocarbon films in aqueous solutions. *Proc. R. Soc. Lond. B Biol. Sci.* **281:**377.

HART, J., E. CHENEY, C. LAWSON, H. MAEHLY, C. MESZTENYI, J. RICE, H. THATCHER, and C. WITZGALL. 1968. Computer Approximations. John Wiley & Sons, Inc., New York.

HODGKIN, A. L., and S. NAKAJIMA. 1972 *a*. The effect of diameter on the electrical constants of frog skeletal muscle fibres. *J. Physiol. (Lond.).* **221:**105.

HODGKIN, A. L., and S. NAKAJIMA. 1972 *b*. Analysis of the membrane capacity in frog muscle. *J. Physiol. (Lond.).* **221:**121.

JACK, J. J. B., D. NOBLE, and R. W. TSIEN. 1973. Electric Current Flow in Excitable Cells. Clarendon Press, Oxford. In press.

LEUNG, J. G-M. 1973. Excitation-contraction coupling of frog skeletal muscle fibers. Ph.D. Dissertation, University of California, Los Angeles.

MARQUARDT, D. W. 1963. An algorithm for least squares estimation of nonlinear parameters. *SIAM (Soc. Ind. Appl. Math.) J. Appl. Math.* **11**:431.

MOBLEY, B. A., W. H. FREYGANG, and R. GUNN. 1973. Reactance of the myoplasm of frog skeletal muscle. *Biophys. Soc. Annu. Meet. Abstr.* **13**:195 *a*.

National Bureau of Standards. 1947. Tables of the Bessel Functions $J_0(z)$ and $J_1(z)$ for complex arguments. Columbia University Press, New York, 2nd edition.

PALTI, Y., and W. J. ADELMAN, JR. 1969. Measurement of axonal membrane conductance and capacity by means of a varying potential control voltage clamp. *J. Membrane Biol.* **1**:431.

PEACHEY, L. D. 1965. The sarcoplasmic reticulum and transverse tubules of the frog sartorius. *J. Cell Biol.* **25** (3, Pt. 2):209.

PEACHEY, L. D. 1973. Electrical events in the T-system of frog skeletal muscle. *Cold Spring Harbor Symp. Quant. Biol.* **87**:479.

PEACHEY, L. D., and R. H. ADRIAN. 1973. Electrical properties of the transverse tubular system. *In* Structure and Function of Muscle G. Bourne, editor. 2nd edition. In press.

PESKOFF, A., and R. EISENBERG. 1973. Interpretation of some microelectrode measurements of electrical properties of cells. *Ann. Rev. Biophys. Bioeng.* **2**:65.

PESKOFF, A., R. S. EISENBERG, and J. D. COLE. 1972. Potential induced by a point source of current in the interior of a spherical cell. *UCLA Engr. Report* No. 7259. 1.

PESKOFF, A., R. S. EISENBERG, and J. D. COLE. 1973. Potential induced by a point source of current inside an infinite cylindrical cell. *UCLA Engr. Report* No. 7303. 1.

SCHNEIDER, M. F. 1970. Linear electrical properties of the transverse tubules and surface membrane of skeletal muscle fibers. *J. Gen. Physiol.* **56**:640.

Scientific Time Sharing, 1971. APL*PLUS Newsletter No. 1. Scientific Time Sharing Corp., Bethesda, Md.

VALDIOSERA, R., C. CLAUSEN, and R. S. EISENBERG. 1973 *a*. The measurement of the impedance of frog skeletal muscle fibers. *Biophys. J.* **14**:295.

VALDIOSERA, R., C. CLAUSEN, and R. S. EISENBERG. 1974 *b*. Impedance of frog skeletal muscle fibers in various solutions. *J. Gen. Physiol.* **63**:460.

VAN DYKE, M. 1964. Perturbation Methods in Fluid Mechanics. Academic Press, Inc., New York.

WATSON, G. N. 1944. Theory of Bessel Functions, 2nd Edn. Cambridge University Press, New York.

WEINBERG, A. M. 1942. Green's functions in biological potential problems. *Bull. Math. Biophys.* **4**:107.